Study of AI combustion operating region of a small two–stroke engine

JanithaWijesinghe, Guang Hong
University of Technology, Sydney

Abstract: Limited load region is one of the main problems of HCCI. In the work reported in this paper the auto–ignition (AI) load region specific to a small two–stroke engine has been investigated. Our objective was to gain a better understanding regarding the characteristics of AI operating regime by studying combustion stability and exhaust emissions. AI combustion was achieved by trapping hot exhaust gases inside the cylinder with an exhaust throttle valve. The intake throttle, exhaust throttle and fuelling rate were manually adjusted to obtain the required engine operating points. The nature of combustion and implications of exhaust emissions have been discussed in relation to the load regions of AI operation. The operation of AI in the medium to high load ranges demonstrated a higher degree of cyclic stability. In contrast to this, AI operation at lower loads demonstrated a higher degree of cyclic instability.

Keywords: Auto-ignition, HCCI, two-stroke engines

INTRODUCTION

Homogeneous charge compression ignition (HCCI) is a novel combustion technology based on the principle of auto–ignition. It combines the benefits of conventional spark ignition (SI) and compression ignition (CI) engines and has been recognized to offer very low levels of fuel consumption and enormous reductions in CO and NO_X emissions. Over the past two decades, HCCI has attracted the interest of the research community for its advantages. Much focus was given to investigate and improve certain limitations of HCCI, so that its benefits could be incorporated into future powertrains.

Controlling the start of combustion and a limited operating range are such challenges of HCCI that have been the focus of improvement.

According to the concept of HCCI, combustion is initiated through auto–ignition (AI) of a near homogeneous air–fuel mixture. Previous in-cylinder visualisation experiments have shown the fact that AI occurs at multiple sites within the combustion chamber as the mixture is compressed by the piston [1]. Along with the compression, the constituting chemicals in the mixture participate in a series of chemical reactions causing a further increase of temperature and pressure. When the minimum temperature required for AI is reached, combustion would take place over the entire volume of the cylinder. As such, HCCI combustion is dominated by chemical–kinetics rather than flame propagation and turbulence effects as in conventional SI or CI combustion processes [2, 3].

In an SI engine with limited compression ratio, the mixture temperature may not rise to a sufficient level to generate AI at the end of the compression stroke. The most practical method to obtain the required thermal energy to trigger AI is to use large quantities of recirculated exhaust gas [4,5]. The amount of residual gas could be as much as 50% of the overall gases inside the cylinder [6]. The earliest reported HCCI researches were mainly focused on two–stroke engines due to their simplicity as well as intrinsic high residual gas rate. Transfer duct throttling and exhaust throttling have been the most common techniques used in conjunction with two–stroke engines to trigger AI [1,7,8]. With the introduction of advanced valve actuation technologies, four–stroke engines became the subject of extensive HCCI research. New valve actuation strategies were adopted to retain large quantities of exhaust gas. Based on these new valve actuation techniques, strategies for HCCI such as early exhaust closing (negative valve overlap) and secondary exhaust opening (re-breathing) are two strategies which have been commonly used in four–stroke related HCCI research [9, 10].

High level of charge dilution caused by the introduction of residual gases in HCCI engines leads to an overall reduction of the in-cylinder temperature during combustion. The low in-cylinder temperature due to the high level of charge dilution in turn leads to a dramatically low level of NO_X emissions.

However, because of the high level of residuals inside the cylinder the achievable maximum brake mean effective pressure (BMEP) was significantly reduced compared to conventional SI and CI engines. In fact, much of the HCCI research has been dedicated to investigate and expand the operating envelop. Various approaches have been taken to extend the limited operating regime of HCCI in both two–stroke engines and four–stroke engines.

Zhao et al. experimentally investigated the application of controlled auto–ignition (CAI) to a four–cylinder four–stroke engine equipped with variable cam shaft timing [5]. CAI was successfully achieved by closing the exhaust valve relatively early during the exhaust stroke and trapping large amounts of hot residual gas. In [5] they presented the range of speed and load within which the CAI was experimentally achieved. From the results a maximum load was established that occurred as a consequence of the valve strategy utilised which limited the breathable air flow. This upper boundary of the CAI envelop was called the gas exchange limit. The maximum CAI limit exhibited a reducing trend for BMEP with the increasing engine speed. A minimum load limit for CAI was also demonstrated. The minimum load was a consequence of reduced exhaust gas temperature. It was reported that the mixture would not auto–ignite because of the low residual gas temperature. Furthermore the mixture could not be ignited using a spark plug because too much exhaust gas was present.

Osborne et al. presented the HCCI operating region obtained from their experimental investigation on a Ricardo flagship two–stroke engine [13]. They recognized that at higher loads the scavenging efficiency increased beyond a point where the residual gas was insufficient to result in auto–ignition. This upper boundary of HCCI was termed as the scavenge limit. At low loads even though large proportions of residual gas was trapped inside the cylinder, the reduced mixture temperature did not allow the occurrence of auto–ignition. From the above cases it is clear that for both two–stroke and four–stroke engines the deterministic factor of the lower load limit is the misfire that occurs from insufficient residual gas temperature.

Wang et al. investigated the effect of SI on HCCI combustion on a gasoline direct injection (GDI) four–stroke engine [14]. They had a focus on HCCI combustion at its critical status (HCCI–CS), which was the status when the mixture temperature and concentration just reached auto-ignition conditions. Their results showed that the stability of HCCI combustion at HCCI-CS was improved by SI and that the transition fluctuations could be reduced by SI when the combustion mode was changed from SI to HCCI. It also showed that the SI triggered global HCCI in the region where misfiring occurred without the spark. It was concluded that the stable HCCI combustion was realized when the mixture temperature and concentration near the top dead centre exceeded HCCI-CS.

This paper reports an experimental study on the AI load region of a small two–stroke engine. Apart from early studies conducted on Activated Radical (AR) combustion, little research has been reported on HCCI on small two-stroke engines in the recent years, especially with regard to the load region. In the present work, the term AI was preferred over HCCI taking into account the possible heterogeneities of the mixture that may occur.

EXPERIMENTAL APPARATUS

Table 1: Engine specification

Engine type	Two-stroke; Loop Scavenged (Schnurle)
Bore	61.5 mm
Stroke	54 mm
Connecting rod length	101.5 mm
Displacement	160 cm^3
No. of transfer ports	2
Trapped compression ratio	6.7:1
Exhaust port opening angle	105.9^o ATDC
Transfer ports opening angle	117.8^o ATDC
Fuel induction system	Intake pipe injection

Figure 1: Experimental apparatus

A 160cc piston ported single–cylinder two-stroke engine was used in this investigation. Its key specifications are listed in Table 1. Figure 1 is the schematic for the basic experimental apparatus set up in the investigation. A hydraulic dynamometer was used to measure the brake torque output of the engine. The cylinder pressure was measured using a PCB 112B pressure transducer and a Kistler 504–E charge amplifier. The pressure data was acquired at every degree of crank rotation with a National Instruments LabView data acquisition system. K–type thermocouples were used to measure the intake and the exhaust temperatures. An Autodiagnostics exhaust gas analyzer was used to measure the HC, CO, CO_2, NO, O_2 and the air to fuel ratio (AFR).

The intake system comprised of an intake manifold with a built-in butterfly valve and a fuel injector as illustrated in Figure 1. The mounting point of the injector on the intake manifold was located between the butterfly valve and the outlet. The intake manifold was designed in such a way that the fuel was injected in the direction of the downstream airflow. Air into the intake manifold was drawn through a heater chamber which had its inlet open to atmosphere. The heater chamber was meant for the purpose of pre-heating the intake air, although not used in the experimental work presented in this paper.

To obtain a homogeneous air and fuel mixture inside the cylinder, gasoline fuel premixed with lubricant oil in a ratio of 40:1, was injected into the intake manifold using a low pressure fuel injector as shown in Figure 1. The fuel injection pressure was 300kPa. The fuel injection was controlled using a PIC micro controller shown by item 12 in Figure 1. An incremental rotary encoder with 360 pulses per revolution was used to determine the instantaneous angular position of the crankshaft. The output of the encoder was used as an external clock to drive the micro controller which determined the SI timing, the fuel injection timing and the width of the fuel injection pulse.

REALISATION OF AI AND AI OPERATING REGION

The temperature of the in-cylinder mixture towards the end of compression is one of the most important factors which determine the occurrence of AI. It was experimentally found that with an unrestricted exhaust port, the minimum inlet air temperature required for AI was approximately 90^0C [15].

Table 2: Approximate exhaust valve restrictions

Valve closing angle	Percentage Restriction
0^0 (fully open)	0
20^0	36
40^0	68
50^0	82
55^0	87
60^0	92

The temperature required for AI was achieved through internal exhaust gas recirculation (EGR), which was facilitated by a butterfly valve installed in the exhaust pipe. The burned gas, trapped by the butterfly valve was in turn mixed with the fresh charge in the following cycle. The item 6 in Figure 1 shows the butterfly valve or the exhaust valve which was installed approximately 20mm downstream from exhaust port. The exhaust butterfly valve was manually adjusted to be between 0^0 and 70^0, where 0^0 indicated the fully-opened valve position and 70^0 the fully–closed valve position. The levels of restriction generated by the exhaust valve at different valve angles are shown in Table 2. The "Percentage Restriction" in Table 2 is defined as the fraction of the valve disk area projected in the axial direction of the exhaust pipe to the cross sectional area of the exhaust pipe. Thus greater exhaust port valve angle means more restriction to the exhaust gas flow. In order to achieve the required AFR,

the intake throttle and the fuel injection pulse width were manually adjusted. In our experiments, when the intake air was at the room temperature of approximately 24^0C, the exhaust valve angle was set in the range of 50^0 to 60^0, providing a restriction of 82% to 92%. The AFR was maintained to be between 16:1 and 17:1.

Figure2: Engine operating regions for AI and SI

Figure 2 illustrates the engine operating regions for SI and AI achieved with internal EGR, in terms of engine speed and the brake mean effective pressure (BMEP). The engine operating conditions with AI are denoted by '◊' and SI by '□'. For both SI and AI, the BMEP and the speed were varied by adjusting the intake throttle and the dynamometer hydraulic resistance. The intake throttle could be manually varied between 10^0 and 90^0 indicating 0% and 100% openings respectively. The percentage opening of the intake throttle was the fraction of the open area projected on the intake pipe cross section. In SI mode, the intake throttle was varied between 20^0 and 90^0 and the exhaust valve was fully open. In AI mode, as the engine operation could not reach the condition with load as low as that in SI mode, the intake throttle was varied between 40^0 and 90^0, while the exhaust valve opening was adjusted between 50^0 and 60^0 to achieve more than 80% restriction as shown in Table 2.

The SI data points shown in Figure 2 were obtained in a condition with a stoichiometric AFR and a fully opened exhaust valve. The AI data points were obtained in a condition with an AFR of 16:1 and an approximate exhaust valve restriction of 80%. The AI upper limit shown in Figure 2 is defined as the maximum BMEP that could be reached in AI mode with the given exhaust valve restriction and AFR. The AI lower limit is where the load becomes too low and as a consequence, the residual exhaust gas temperature becomes insufficient to maintain continuous AI [5]. Misfiring or partially burning cycles are common below the AI lower limit, which make it difficult to maintain AI.

AI COMBUSTION IN MEDIUM TO HIGH OPERATING LOADS

The engine load is presented in terms of BMEP. The shaded area in Figure 2 depicts the medium to high load region discussed in this section. The average exhaust temperature measured in the experiments at medium to high engine load was above 350^0C. Within this load region AI demonstrated a rapid heat release compared to SI operation. Figure 3 compares the rate of heat release in AI operation with that in SI operation. As shown in Figure 3 the main heat release occurred within about 20^0 of crank rotation at 3000RPM and a BMEP of 190kPa. In contrast, the main heat release of SI operation spanned over 40^0 of crank rotation at the same engine speed and load.

Figure 3: Heat release rate for AI and SI at speed-3000RPM and BMEP-190kPa

It was noticed that under AI operation at medium to high engine load, the cycle–to–cycle variation was significantly reduced compared to that of SI operation. This can be seen in Figure 4 by comparing the pressure traces recorded when the engine was operating in AI (a) and SI (b) conditions, where the engine speed and the BMEP were maintained at 3000RPM and 190kPa respectively for both AI and SI operations.

The cycle-to-cycle variation was also quantitatively evaluated by the coefficient of variation (CoV) of the peak cylinder pressure. The CoV was calculated with the following equation:

$$\text{CoV} = \frac{\text{Standard deviation}}{\text{Sample average}} \times 100\% \quad (1)$$

In AI operation, the CoV of the peak cylinder pressure of 25 consecutive engine cycles shown in Figure 4(a) was 1%. In contrast to this, the cylinder pressure in the SI operation as shown in Figure 4(b) resulted in a CoV of 14%.

(a) AI operation

(b) SI operation

Figure 4: Cylinder pressure at speed-3000RPM and BMEP-190kPa under (a) AI operation, (b) SI operation

(a) 10% MBF timing (b) 10% to 90% MBF angle

Figure 5: Ignition timing and duration in AI operation at speed-3000RPM and BMEP-190kPa: (a) 10% MBF timing (b) 10% to 90% MBF angle

In order to determine the onset of AI, mass burned fraction (MBF) was calculated using the cylinder pressure data. The method of calculating the MBF was first introduced by Marvin[16]. It was explained in more detail by Ivansson [17].

The position of the crank with respect to the TDC, when 10% of the fuel mass had burned was considered as the ignition timing. The crank rotation between the events of 10% MBF and 90% MBF was considered as the combustion duration. Figure 5 shows the ignition timing and combustion duration of 15 consecutive cycles of the AI and SI operations in the same engine operating conditions as that in Figure 4. According to Figure 5(b), combustion duration ranged between 9^0 to 10^0. The variation of the combustion duration was small compared to the variation of the combustion timing as shown in Figure 5(a). This may indicate that the required temperature for AI was not achieved exactly at the same position of crank rotation in each successive cycle.

Conventional carburetted two–stroke engines have high HC emissions caused by fuel short circuiting due to the large overlap of the transfer port opening and exhaust port opening. Especially at low speed and high load conditions, the level of HC emissions increases with the decreasing trapping efficiency of the engine. The exhaust pipe valve used for internal EGR not only trapped the exhaust gas to achieve the temperature required by AI but also generated a restriction to reduce fuel short-circuiting. As shown by the fuel consumption and the HC emissions in Figure 6, the use of an exhaust valve to achieve AI

significantly reduced the fuel escaping through the exhaust port and hence reduced the hydrocarbon emissions. For the results shown in Figure 6, the AFR of the mixture used in SI operation was 14, whereas the AFR for AI operation was 16. The leaner mixtures together with the reduced fuel short-circuiting in AI operation led to more than 20% reduction in fuel consumption as shown in Figure 6(a).

(a) BSFC (b) BSHC

Figure 6: Comparison of engine performance in AI and SI operations

(a) BSFC and (b) BSHC at BMEP-200kPa

AI COMBUSTION AT LOWER LOADS

Previous research work has shown that for both two–stroke and four–stroke engines the deterministic factor of the lower load limit was the misfire caused by low residual gas temperature [5, 7]. At the light load conditions less heat was released than that at higher load conditions. Therefore the temperature of the residual gases trapped inside the cylinder at lower loads may not be high enough to result in AI at the end of the compression stroke. The heat loss is another factor that affects AI. The higher ratio of surface area to volume in a small engine results in greater heat loss per cycle. When the heat loss constitutes a large fraction of the total heat release, the in-cylinder temperature becomes too low to achieve AI [1].

With reference to Figure 2 the lower load region discussed in this section is part of the AI region, which is excluded by the shaded area. At lower engine load conditions as shown in Figure 7, the peak pressure in AI operation varies more significantly from cycle–to–cycle than it does at the higher engine load conditions. A smaller pressure rise in one cycle indicates an event of partial combustion that leaves a significant amount of intermediate reactants within the cylinder. In this way the next cycle would have a higher amount of intermediate reactants in the residual gas which would cause the mixture to auto-

ignite with an above average pressure rise. Due to this reason a cycle with a lower peak pressure is always followed by a cycle with a significantly higher peak pressure also seen in Figure 7.

Figure 7: Pressure distribution in AI operation at 3000RPM, AFR-16, and BMEP-155 kPa

Figure 8: Pressure distribution in SI operation at 3000RPM, AFR-16, and BMEP-130 kPa

The CoV for the peak cylinder pressure given in Figure 7 is 13%. Typically the CoV value for stable AI operation observed in the medium load ranges is about 1%. This difference in the CoV values indicates that there is a significant increase in cyclic variability when the AI lower limit is reached. Furthermore, while the engine was operated at the lower load limit of AI, combustion could not be sustained for longer periods. However under the said operating conditions when the spark ignition system was left enabled combustion continued uninterrupted. As explained by Wang et al, in this type of a situation SI would act as a trigger to initiate AI [14]. The heat released to the surroundings by the local flame propagation could increase the temperature of the remaining fresh charge leading to AI.

(a) BSFC (b) BSHC

Figure 9: Comparison of engine performance in AI and SI operations

(a) BSFC and (b) BSHC at BMEP-160kPa

The occurrence and the existence of AI were highly sensitive to variations of the operating conditions under lower load operation. During the experiments it was evident that anything that caused a slight drop in exhaust temperature would cause the AI mode to discontinue. Similarly if the mixture of the AFR was momentarily reduced below a certain threshold (approximately 15 AFR) AI would not occur. During the test runs where spark was continuously supplied, a change in operating conditions caused the engine to change to SI. However when the engine combustion mode changed to SI, the engine speed

also reduced significantly. Since the exhaust gas flow was heavily restricted to suit the AI mode, the fresh charge might still be highly diluted by the trapped exhaust gas. Therefore the flame propagation would not have occurred effectively, causing this reduction of speed under the SI mode. The pressure trace shown in Figure 8 depicts such an instance of SI operation. In the pressure trace shown in Figure 8 a periodic pattern could be observed, where a high in-cylinder pressure peak occurred continuously after every two successive low pressure peaks. The lower pressure peaks represent cycles that partially ignited due to poor flame propagation. However after two successive cycles of incomplete combustion the mixture in the third cycle may have become sufficiently rich from the accumulated residue to result in a more completely burned cycle. In this mode a definite reduction in combustion efficiency is inevitable as a consequence of high cyclic instability.

Figure 9(a) depicts the fuel consumption obtained at a constant load of 160kPa which lies near the lower load limit of AI. According to these results a 17% to 23% improvement is shown in AI operation compared to SI operation. However an appreciable reduction in HC emissions cannot be seen in Figure 9(b) under AI operation. On the other hand by comparing Figure 6(b) and Figure 9(b) a reduction of HC emissions under SI operation could be seen in the latter. The corresponding exhaust valve restrictions for SI and AI operations shown in Figure 9 were 68% and 87% respectively. Therefore the restriction applied by the exhaust valve in SI operation is lower compared to that in AI. As such it could be inferred that it is the part throttle operation which leads to the reduction of HC emissions in SI mode. Furthermore the main reason for the reduction in fuel consumption in AI mode shown in Figure 9 is the use of a lean AFR.

CONCLUSIONS

Characteristics of AI under different load conditions were experimentally investigated in a small two-stroke single cylinder engine equipped with an exhaust valve to generate auto-ignition. After studying the cylinder pressure and exhaust emissions data the following conclusions were reached.

1. Under the investigated conditions AI was achieved within the speeds of 2000RPM to 3200RPM and BMEP in a range of 150kPa to 250kPa. The upper load limit was reached along with the gas exchange limit due to the exhaust valve restriction. The lower load limit occurs as a result of insufficient combustion temperatures to manifest AI. The corresponding AFR had to be maintained within lean limits of 16:1 to 17:1.
2. At medium to high loads, AI combustion demonstrated a significantly lower variation of peak cylinder pressure compared to that of SI combustion. The CoV of AI was 1% whereas the CoV of SI was 14%.
3. At medium loads, the crankshaft rotation angle between 10% and 90% MBF events was relatively stable, compared to the variation of the 10% MBF angle.
4. The AI operation at medium loads was characterised with approximately 20% reduced fuel consumption and 30% reduced HC emissions with respect to SI operation.
5. At lower loads AI combustion suffered from insufficient exhaust temperatures. Compared to that of medium load regions the variation of peak pressure of AI lower loads was much higher.
6. Lower load operation did not lead to a significant reduction in HC emissions with respect to that of SI operation, although a 17% to 23% drop in fuel consumption was achieved in AI mode.

REFERENCES

[1] Shigeru Onishi, Souk Hong Jo, Katsuji Shoda, Pan Do Jo, and Satoshi Kato. Active thermo-atmosphere combustion (ATAC) - A new combustion process for internal combustion engines. SAE paper 790501, 1979.

[2] J. A. Eng, W. R. Leppard, and T. M. Sloane. The effect of PO_x on the autoignition chemistry of n-heptane and isooctane in an HCCI engine. SAE Paper 2002–02–2861, 2002.

[3] Jincai Zheng, Weiying Yang, David L. Miller, and Nicholas P. Ceransky. A skeletal chemical kinetic model for the HCCI combustion process. SAE Paper 2002–01–0423, 2002.

[4] Paul M. Najt and James A. Eng. Homogeneous Charge Compression Ignition (HCCI) Engines: Key Research and Development Issues, chapter Gasoline–Fuelled HCCI Engines, pages 1–144. Society of Automotive Engineers, 2003.

[5] H. Zhao, J. Li, T. Ma, and N. Ladommatos. Performance and analysis of a 4–stroke multi-cylinder gasoline engine with CAI combustion. SAE paper 2002–01–0420, 2002.

[6] Roy Ogink. Computer Modeling of HCCI Combustion. PhD thesis, Division of Thermo and Fluid Dynamics, Chalmers University of Technology, Sweden, 2004.

[7] Y. Ishibashi. Basic understanding of activated radical combustion and its two-stroke engine application and benefits. SAE paper 2000-01-1836, 2000.

[8] R. Gentill, S. Frigo, F. Cozzolino, and S. Zanforlin. Influence of engine parameters on ATAC behaviour in a G.D.I two–stroke engine. Dipartimento di Energetica–Universit`a di Pisa, 2001–01–1858/4275, 2001.

[9] A. Babajimopoulos, G. A. Lavoie, and D. N. Assanis. Modeling HCCI combustion with high levels of residual gas fraction – a comparison of two VVA strategies. SAE paper 2003–01–3220, 2003.

[10] Jeff Allen and Don Law. Variable valve actuated controlled auto-ignition: Speed load maps and strategic regimes of operation. SAE paper 2002–01–0422, 2002.

[11] J. Yang. Expanding the operating range of homogeneous charge compression ignition spark ignition dual-mode engines in the homogeneous charge compression ignition mode. International Journal of Engine Research, IMechE, 6:279–288, 2005.

[12] Fuquan Zhao and Thomas W. Asmus. Homogeneous Charge Compression Ignition (HCCI) Engines: Key Research and Development Issues, chapter HCCI Control and Operating Range Extension, pages 323–420. Society of Automotive Engineers, 2003.

[13] R. J. Osborne, G. Li, S. M. Sapsford, J. Stokes, T. H. Lake, and M. R Heikal. Evaluation of hcci for future gasoline powertrains. In Homogeneous Charge Compression Ignition (HCCI) Combustion 2003, pages 109–126. SAE paper 2003–01–0750, 2003.

[14] Z. Wang, J. Wang, S. Shuai, G. Tian, X. An, and Q. Ma. Study of the effect of spark ignition on gasoline hcci combustion. Proceedings of IMechE, Part D: Journal of Automobile Engineering, 220:817–825, 2006.

[15] Janitha Wijesinghe and Guang Hong. Using auto-ignition to improve the cycle-to-cycle variations of a small two-stroke engine. SAE paper 2007–32–0040, 2007.

[16] C. F Marvin. Combustion time in the engine cylinder and its effects on engine performance. Technical report, NACA, 1927.

[17] N. Invansson. Estimation of the residual gas fraction in an hcci-engine using cylinder pressure. Master's thesis, Vehicular Systems, Department of Electrical Engineering, Linkping University, Sweden, 2003

Figure 1

Click here to download high resolution image

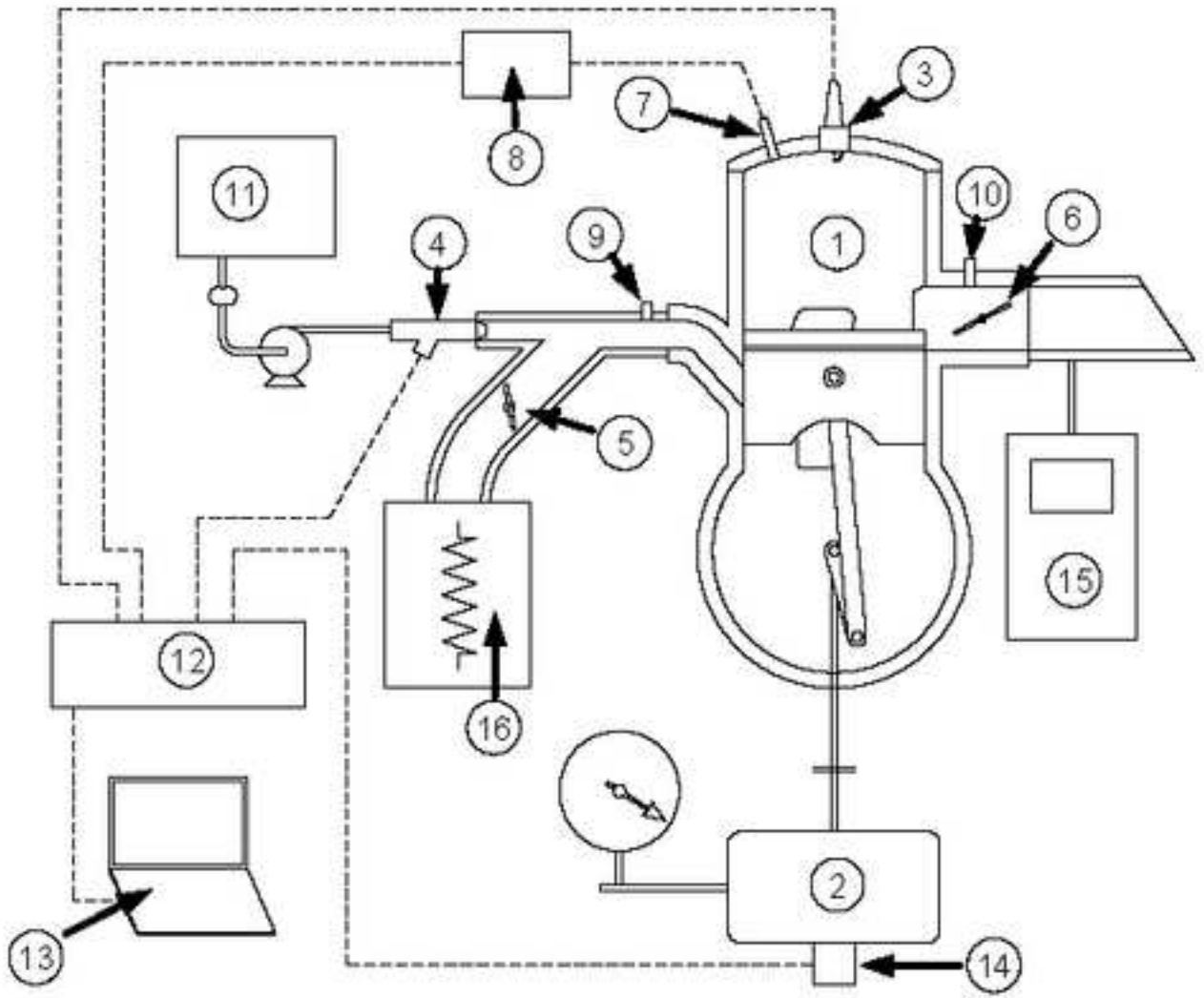

1-Test engine 2-Dynamometer 3-Spark plug 4-Fuel injector 5-Intake valve 6-Exhaust valve 7-Pressure transducer 8-Charge amplifier 9-Intake thermocouple 10-Exhaust thermocouple 11-Fuel supply system 12-Microcontroller 13-Data acquisition computer 14-Incremental rotary encoder 15-Exhaust gas analyzer 16-Intake heater chamber

Figure 2

Click here to download high resolution image

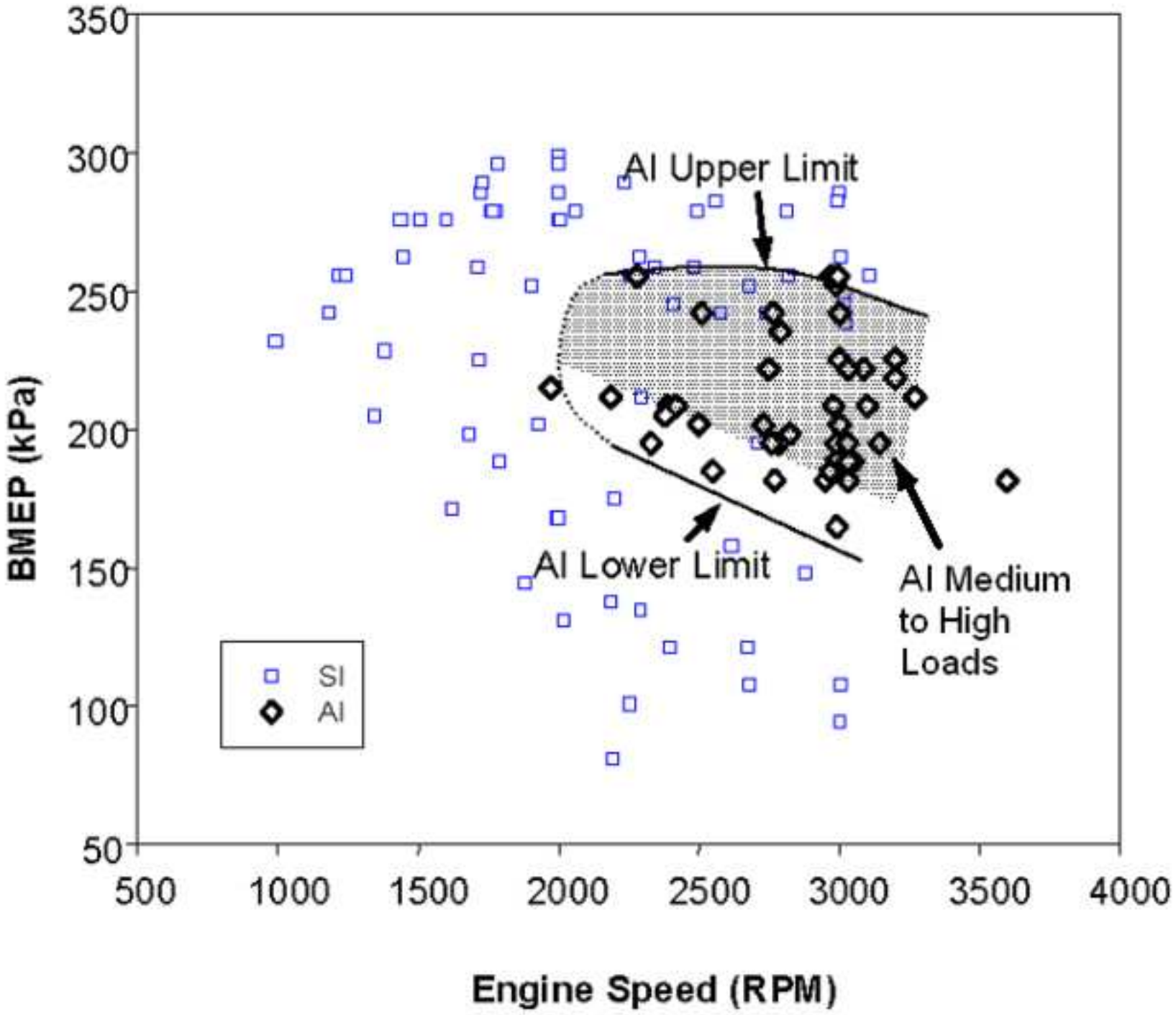

Figure 3

Click here to download high resolution image

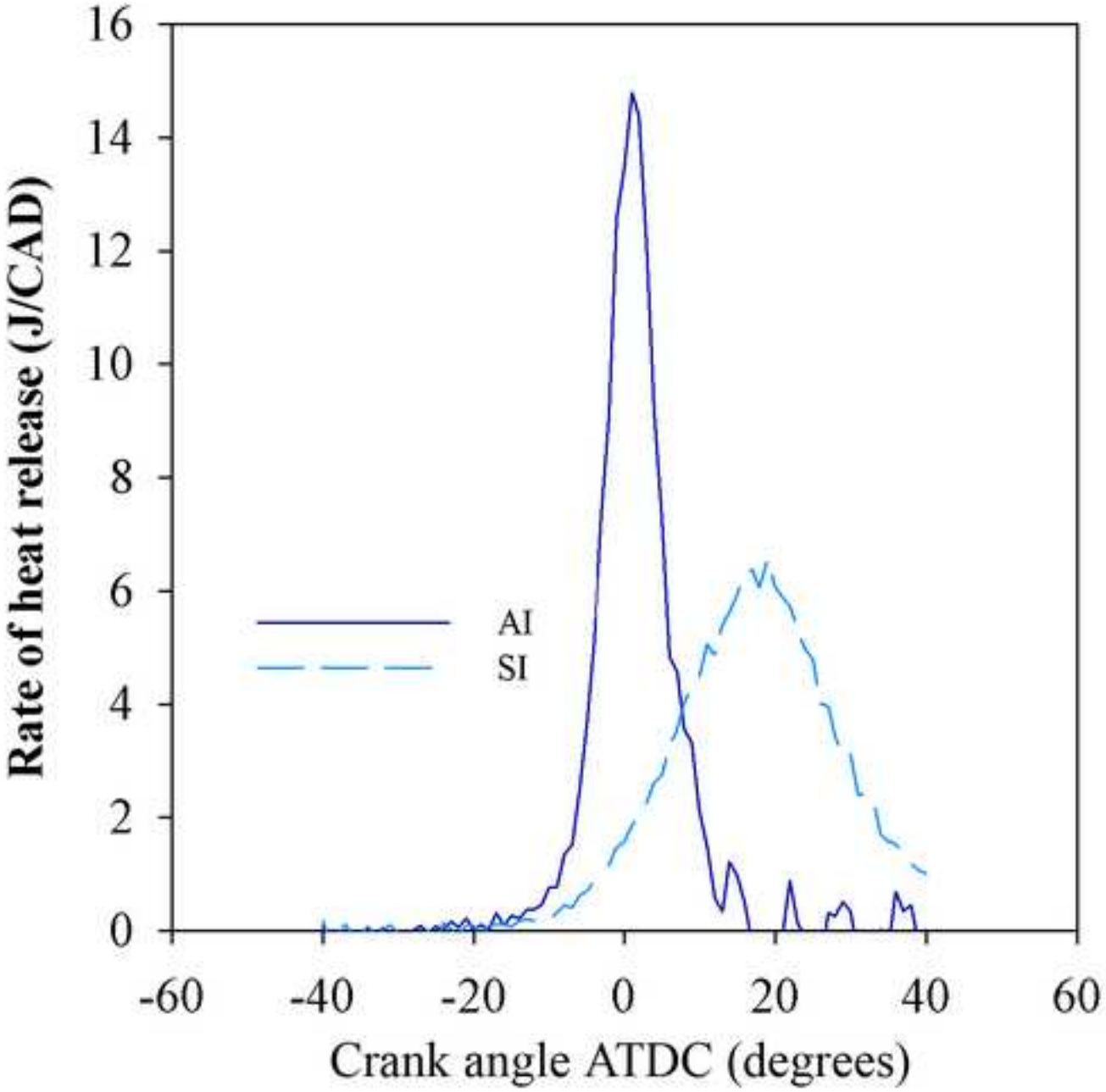

Figure 4a

Click here to download high resolution image

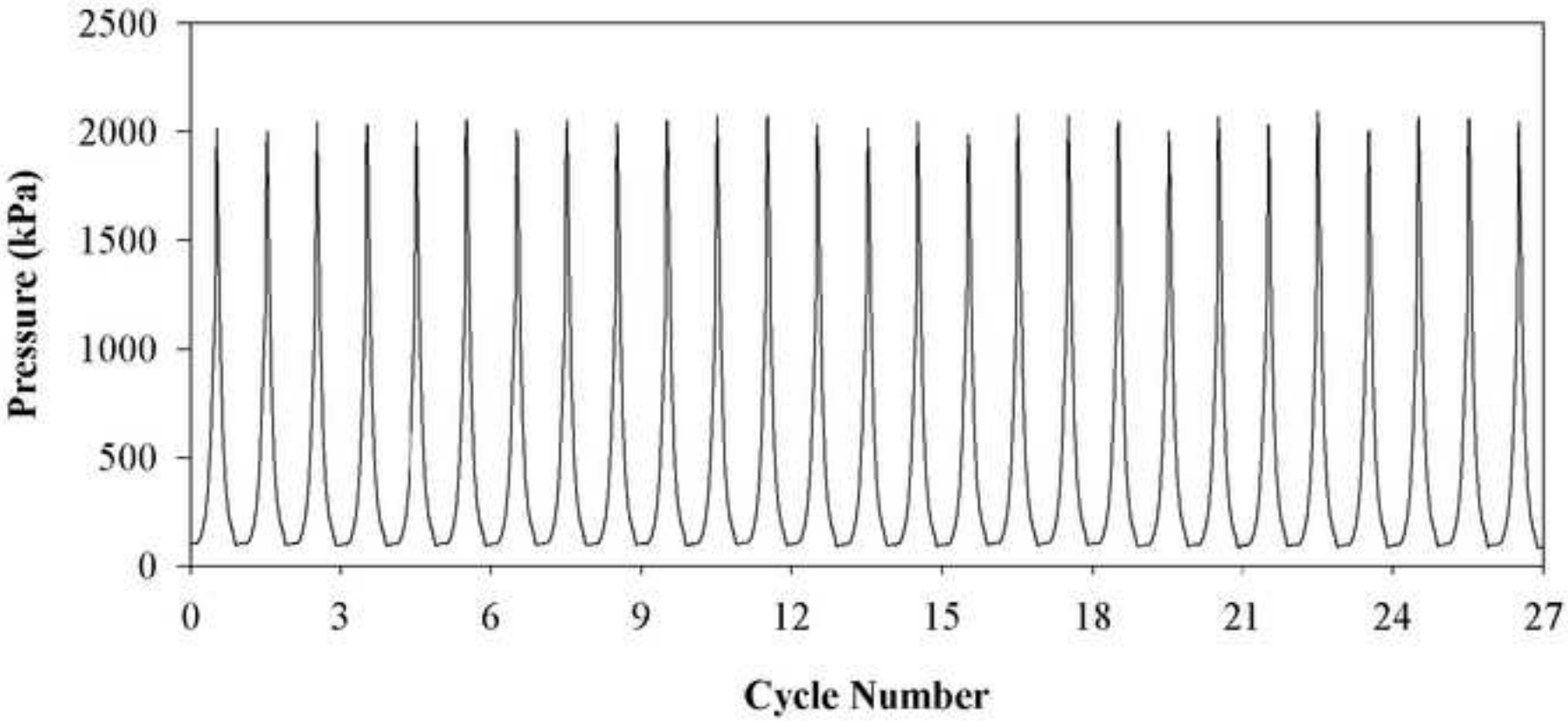

Figure 4b
Click here to download high resolution image

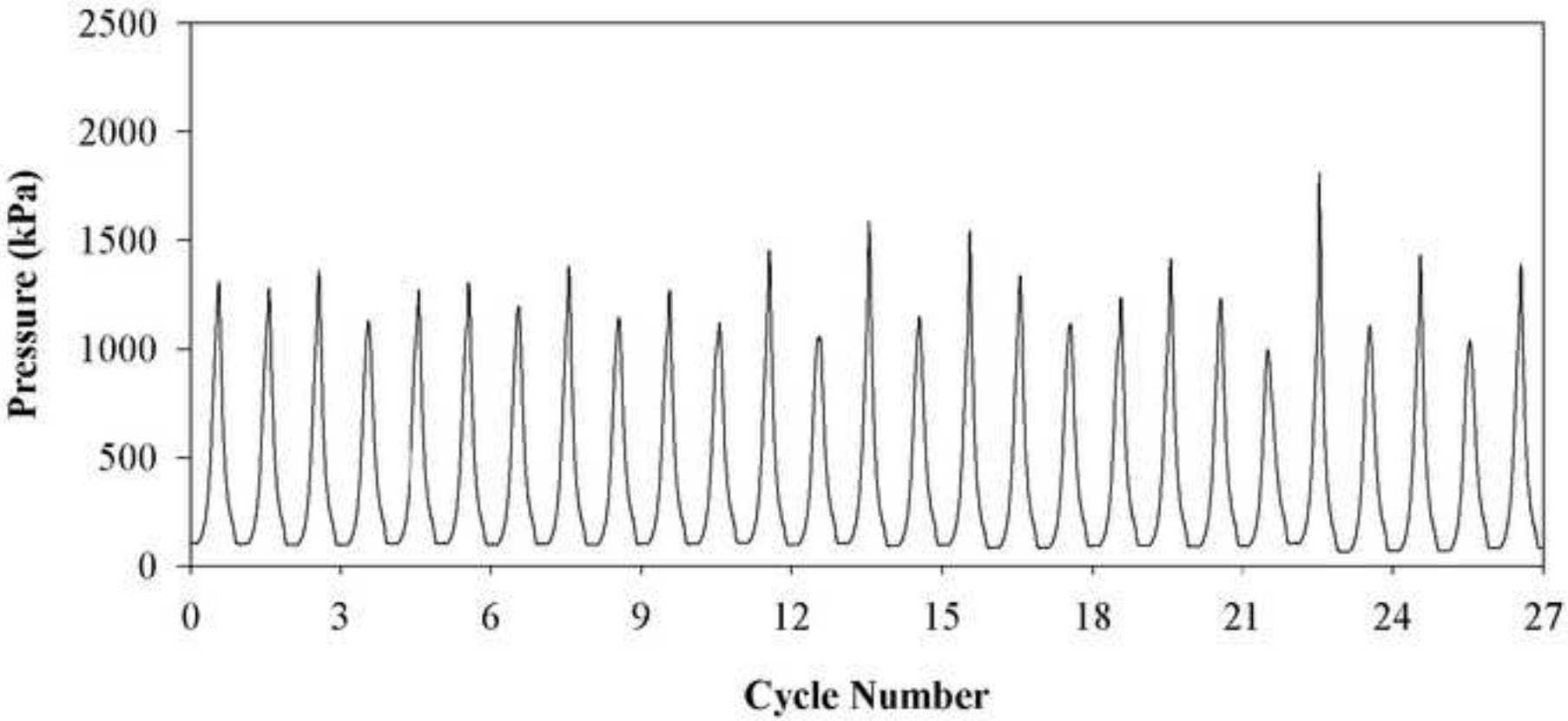

Figure 5a

Click here to download high resolution image

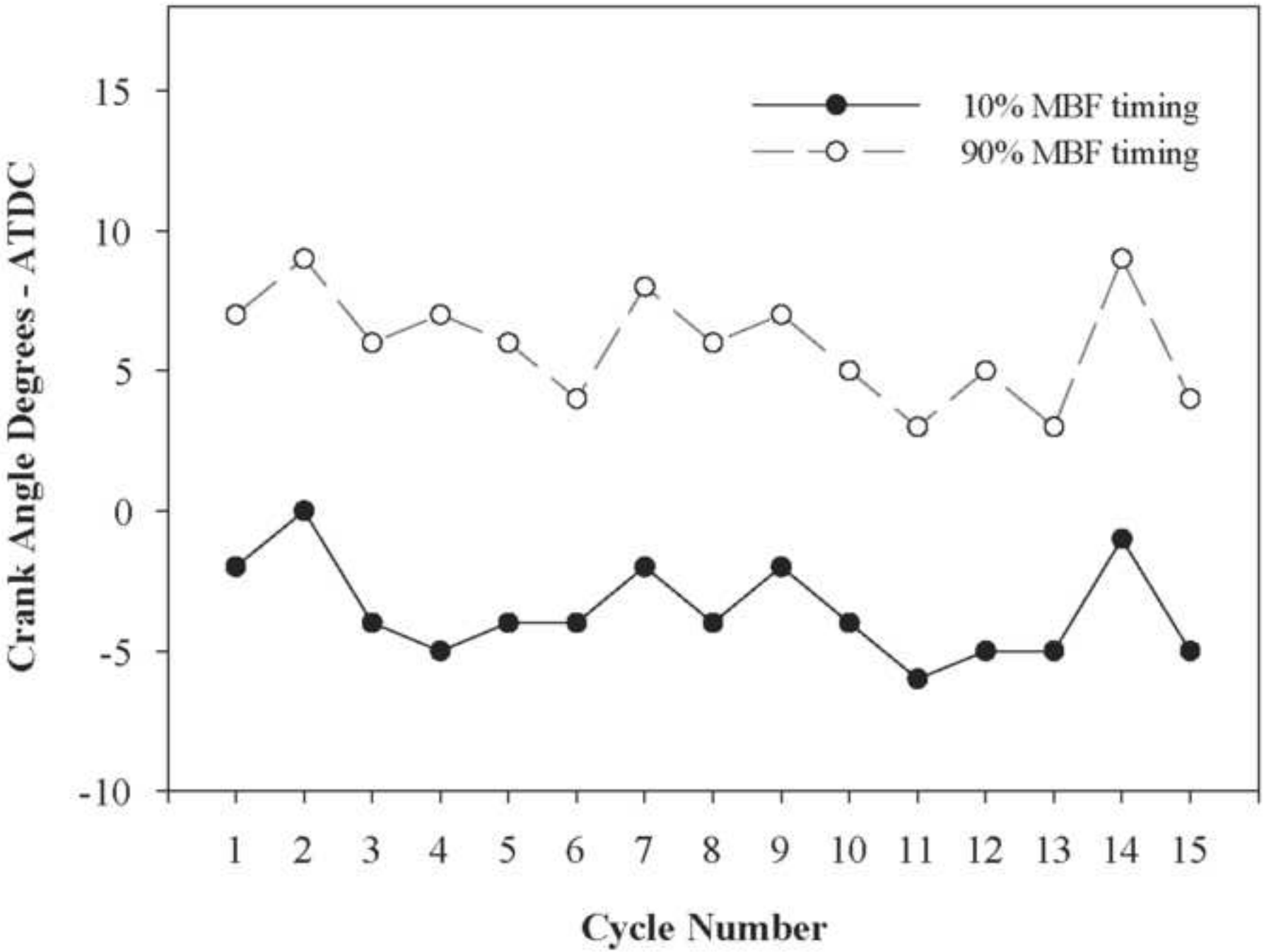

Figure 5b
Click here to download high resolution image

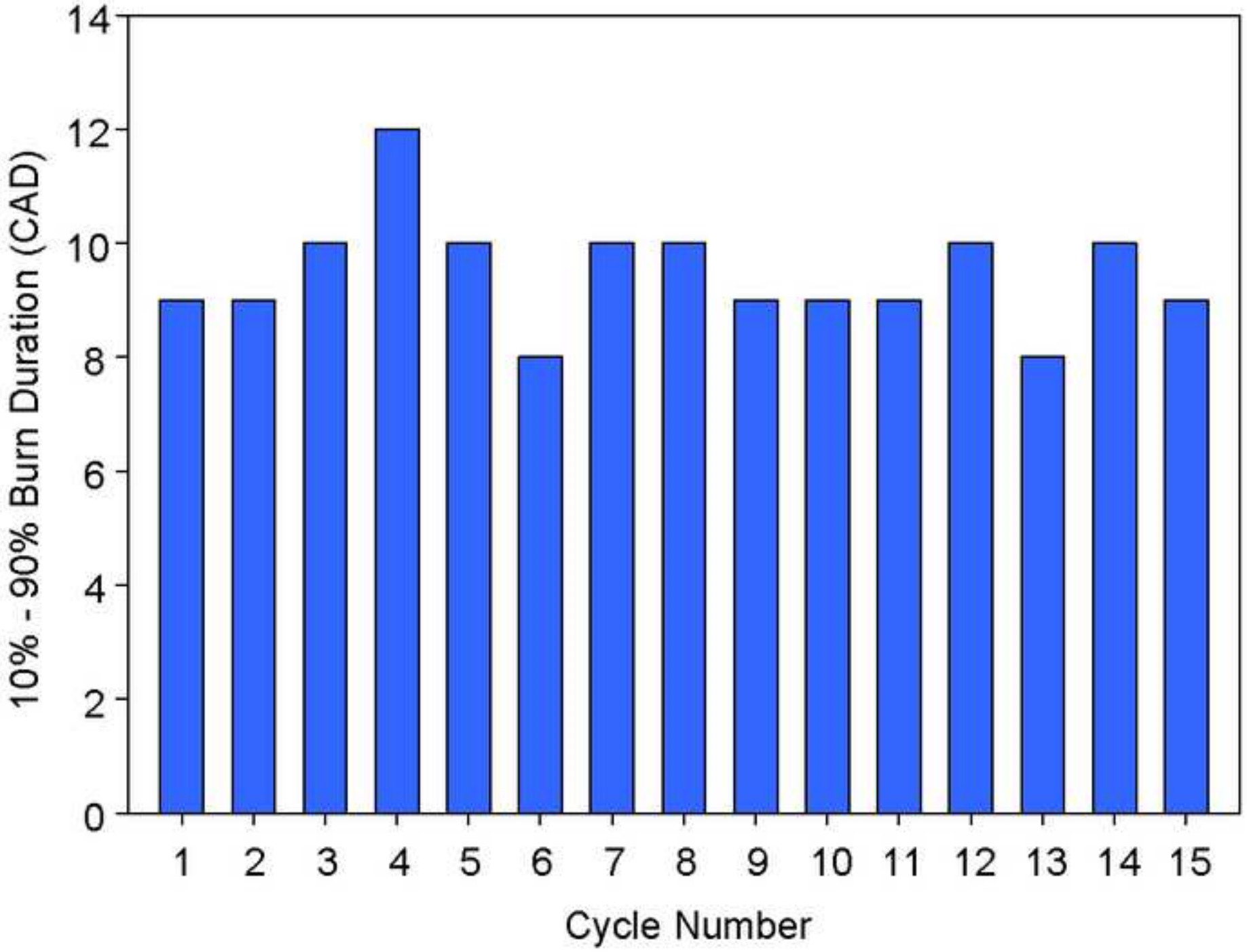

Figure 6a
Click here to download high resolution image

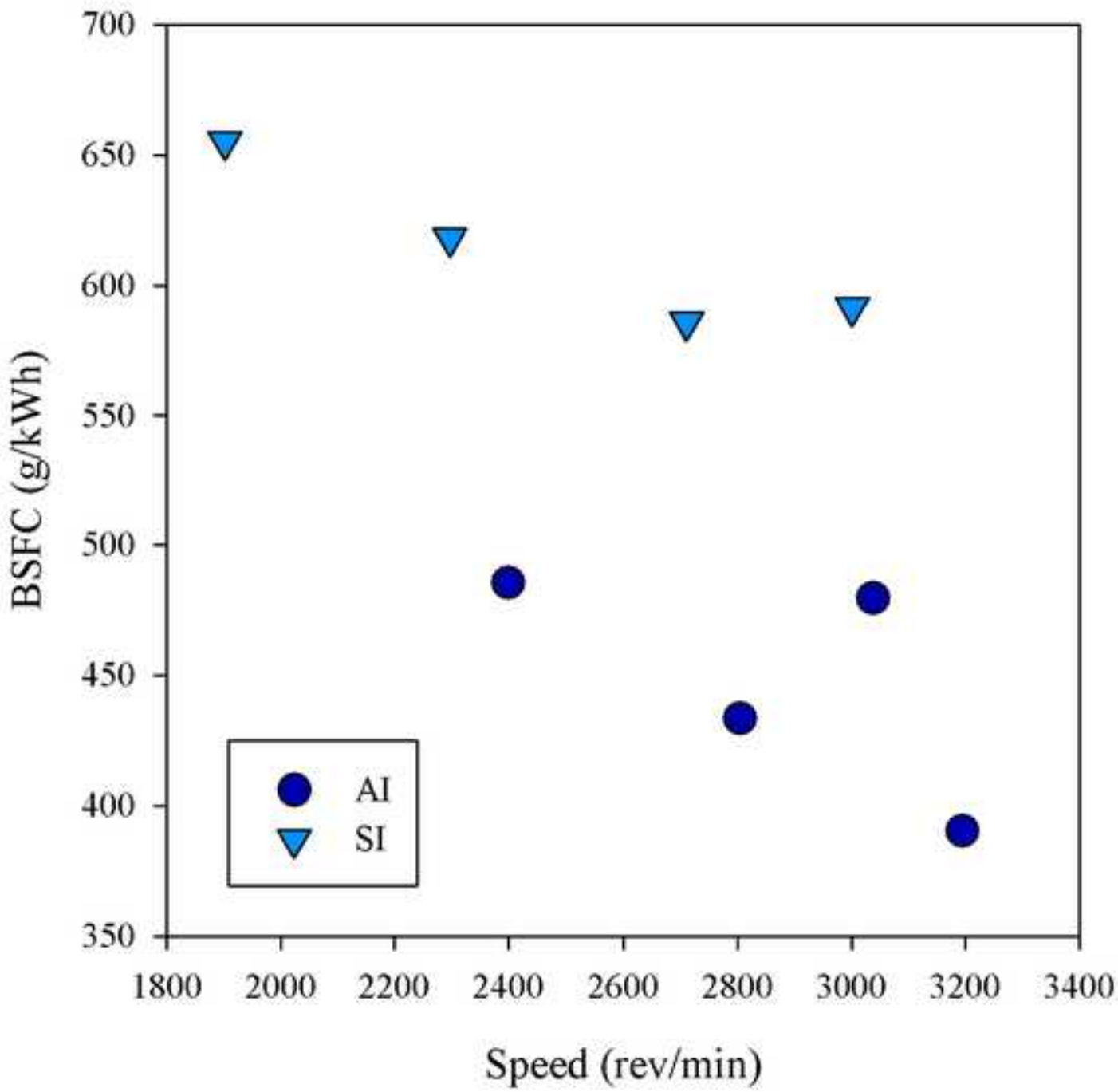

Figure 6b

Click here to download high resolution image

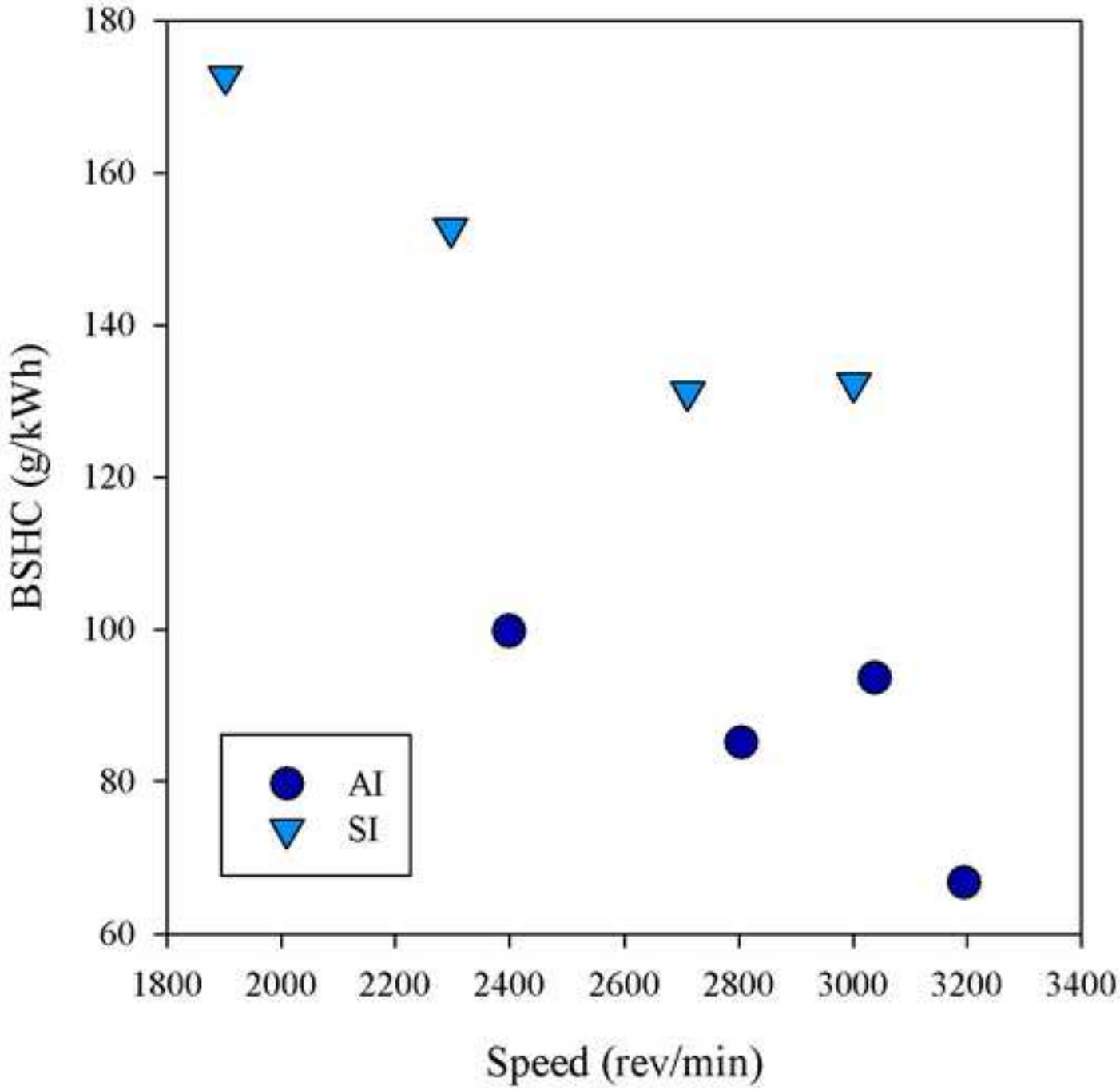

Figure 7

Click here to download high resolution image

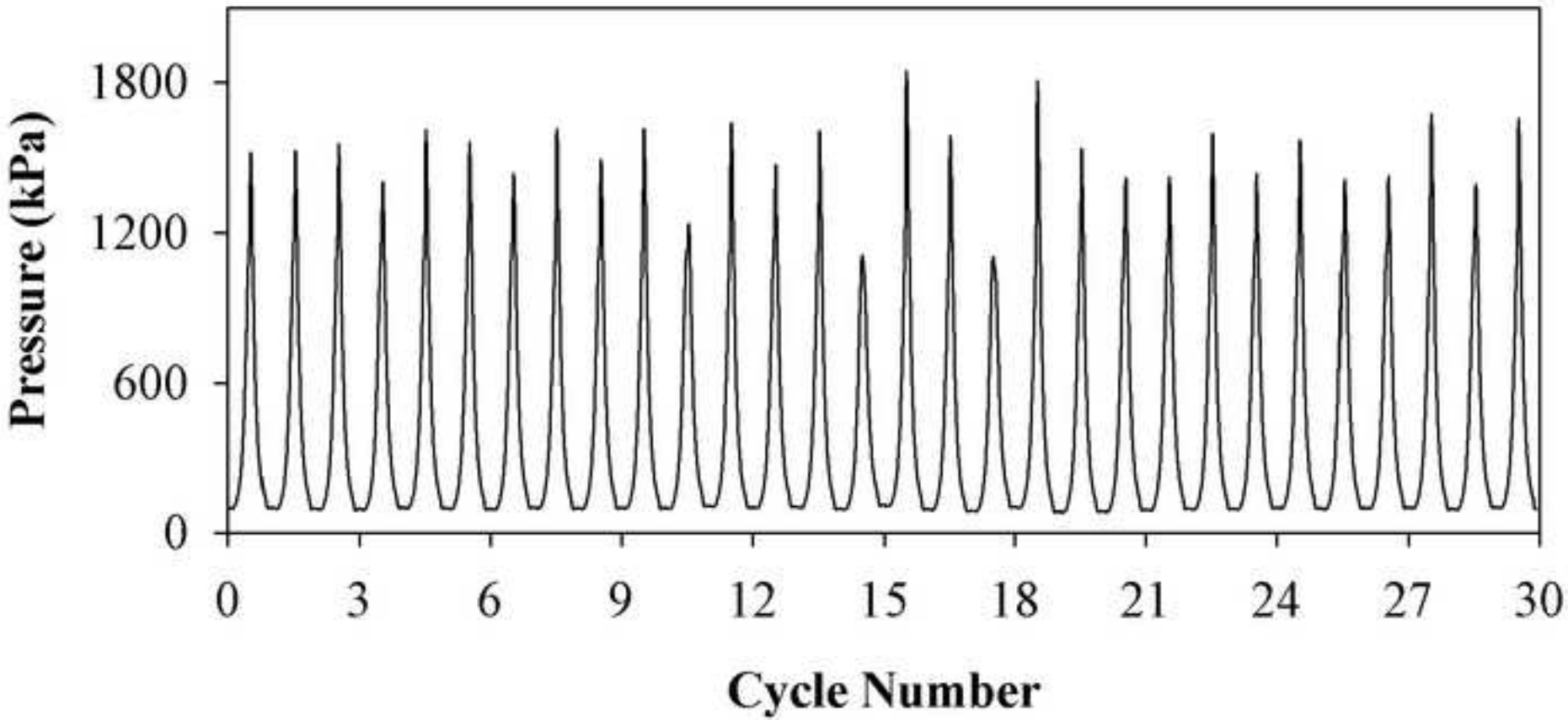

Figure 8

Click here to download high resolution image

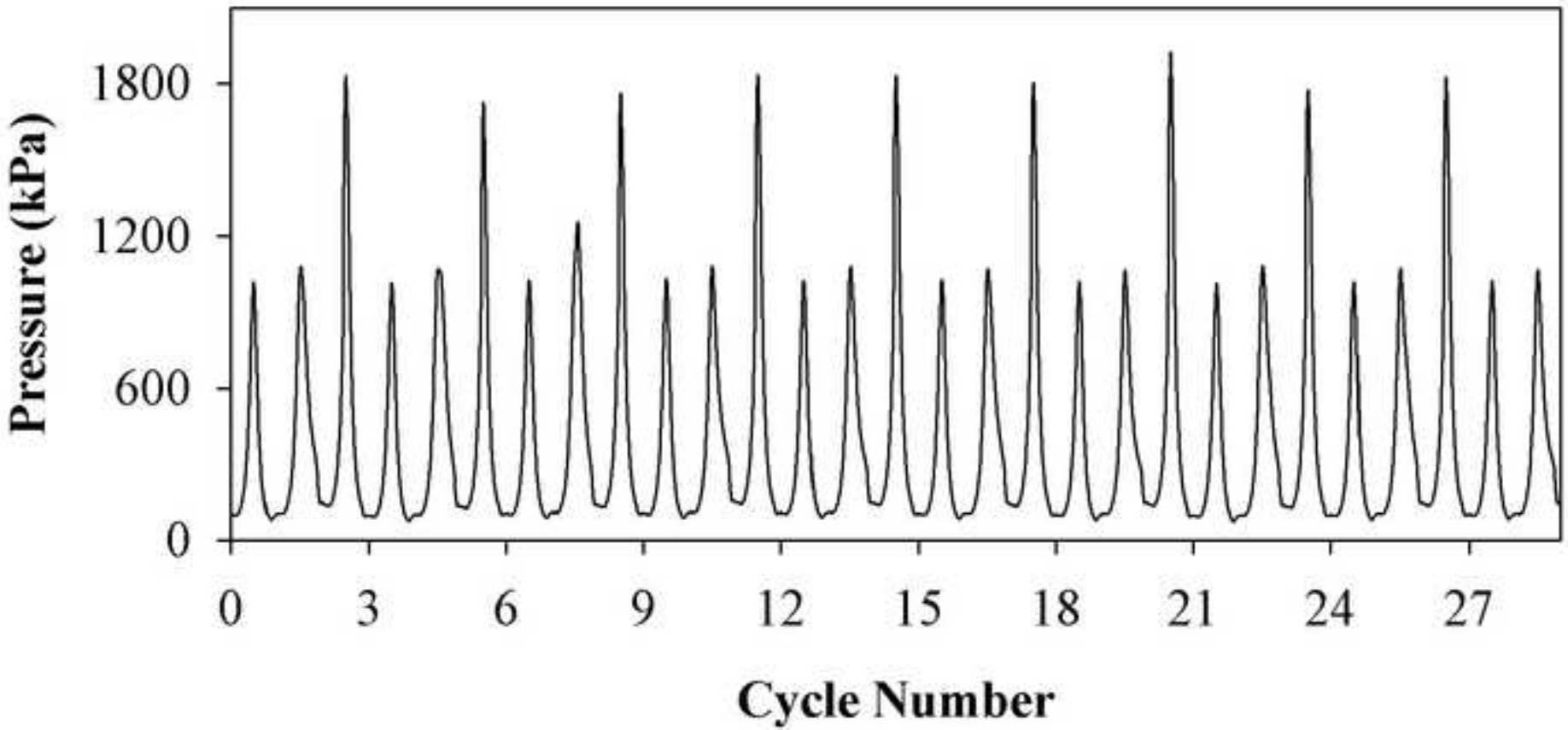

Figure 9a
Click here to download high resolution image

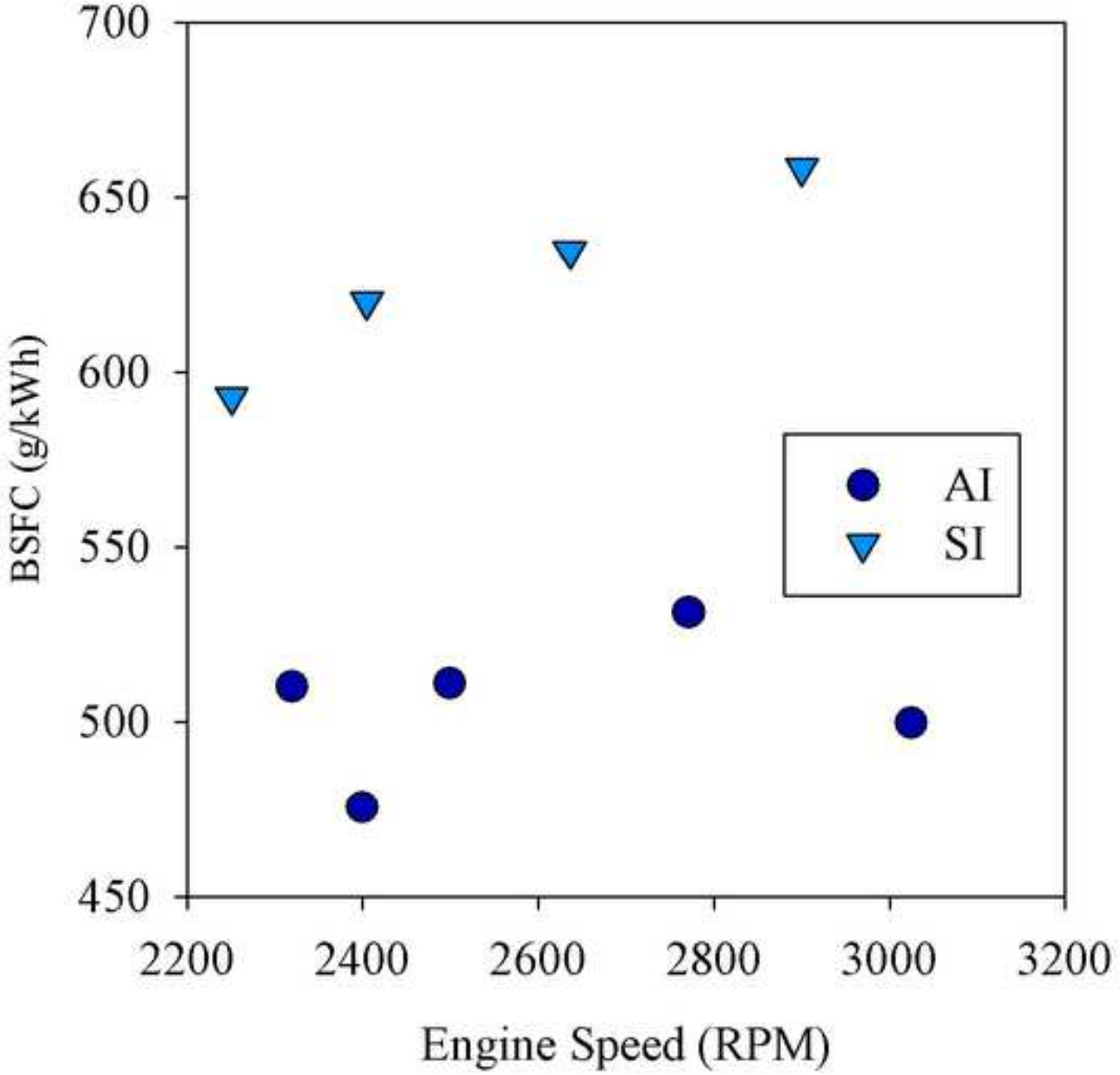

Figure 9b
Click here to download high resolution image